Observation of Quadratic Fermi Node in a 3D Strongly Correlated Semimetal

Strong spin-orbit coupling fosters exotic electronic states such as topological insulators and superconductors, but the combination of strong spin-orbit and strong electron-electron interactions is just beginning to be understood. Central to this emerging area are the 5*d* transition metal iridium oxides. Here, in the pyrochlore iridate $Pr_2Ir_2O_7$, we identify a non-trivial state with a single point Fermi node protected by cubic and time-reversal symmetries, using a combination of angle-resolved photoemission spectroscopy and first principles calculations. Owing to its quadratic dispersion, the unique coincidence of four degenerate states at the Fermi energy, and strong Coulomb interactions, non-Fermi liquid behavior is predicted. Our discovery implies that $Pr_2Ir_2O_7$ is a parent state that can be manipulated to produce other strongly correlated topological phases, such as topological Mott insulator, Weyl semi-metal, and quantum spin and anomalous Hall states.

Following the discovery of topological insulators [1–4], the next frontier is the regime in which both spin-orbit coupling and correlation effects are strong [5–11]. Theory has suggested that the pyrochlore iridates, a family of cubic 5*d* transition metal oxides [12, 13], may realize both band inversion, the essential ingredient of topological insulators, and strong correlations [8, 11]. Empirical evidence for the latter is plentiful. Notably, $Pr_2Ir_2O_7$ appears to be proximate to an interaction-driven antiferromagnetic quantum critical point tuned by A site ionic radius, which is located between the two ions with largest radii, A = Pr and A = Nd [13, 14]. It is the only compound among the series in which the iridium electrons remain paramagnetic and itinerant down to the lowest measured temperatures. It displays "bad metallic" behavior and nontrivial spontaneous Hall transport, suggesting strong correlations [6, 14, 15]. Moreover, recent thermodynamic measurements have revealed zero-field quantum criticality without tuning [16].

The phenomenological suggestion of Ref. [10], whose implications are summarized in **Fig. 1**, is that the Fermi surface of $Pr_2Ir_2O_7$ contains a single Fermi node at the Γ point, which emerges as the touching point of two quadratically dispersing "conduction" and "valence" bands [17]. The presence of this touching is actually required by symmetry and group theory (the quadruplet at the zone center lies in the Γ_8 representation of the double group of O_h), but its location directly at the Fermi energy was an ad-hoc theoretical assumption. If the assumption is correct, $Pr_2Ir_2O_7$ becomes a strongly correlated analog of HgTe [18, 19], which has a mathematically identical quadratic node at the Fermi energy, and implies that $Pr_2Ir_2O_7$ should be tunable into various topological states (see **Fig. 1**). Furthermore, theory has predicted that the quadratic nodal semimetal itself is fundamentally altered by long-range Coulomb interactions (negligible in HgTe due to the large dielectric constant, but not so here), becoming a non-Fermi liquid state. Thus the Fermi node, if correct, means that $Pr_2Ir_2O_7$ is a natural parent material for strongly interacting topological phases and non-Fermi liquid states.

Angle-resolved photoemission spectroscopy is a powerful technique to directly observe the electronic structure of matter. One incident photon energy corresponds to one k_z value in solid, thus the momentum space observed at a fixed photon energy is limited to a k_x-k_y plane at a fixed k_z (**Fig. 2a**). To locate the Γ-point, therefore, sweeping the photon energy is required. In order to observe the Fermi node, we measured the ARPES spectra at various photon energies. The observed momentum cut shifts with photon energy along the $k_{(111)}$ axis within a momentum sheet crossing the Γ, L, and K points. The most significant finding is that the

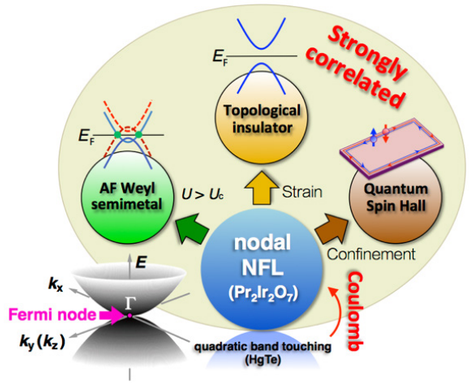

Figure 1: Quadratic Fermi node state of $Pr_2Ir_2O_7$ tunable into interacting topological phases. In the lower part of the diagram, the bottom half of the blue circle and its reflection form a caricature of the quadratically dispersing conduction and valence bands touching at the zone center, while at the same time the darker blue upper circle suggests how $Pr_2Ir_2O_7$, with non-negligible Coulomb interactions, is a strongly correlated non-Fermi liquid analog of HgTe, shown as a pale blue reflection. Arrows indicate the perturbations which convert the nodal non-Fermi liquid (NFL) state to diverse topological phases: an antiferromagnetic Weyl semimetal should be produced in bulk materials by alloying or hydrostatic pressure, uniaxial strain yields a three-dimensional topological insulator, and two-dimensional confinement produces a quantum spin Hall state. The outer circle reminds us that all the states produced in these ways retain strong correlations, and hence are excellent candidates for observing non-trivial surface phases different from those of band theory, as discussed in the text.

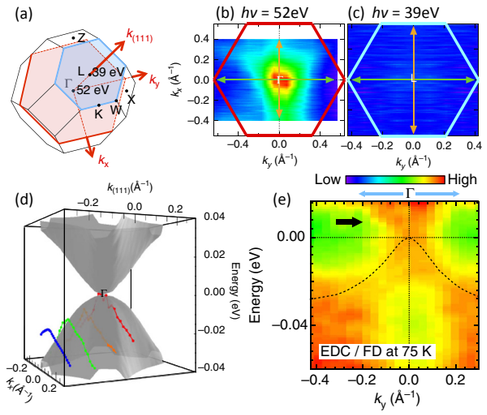

Figure 2: (a) Brillouin zone of $Pr_2Ir_2O_7$. **(b, c)** ARPES intensity map at E_F across Γ and L, measured at $h\nu$ = 52 eV and 39 eV, respectively. The corresponding momentum sheets are indicated in **(a)** with red and blue colors. **(d)** Band calculation for $Pr_2Ir_2O_7$ showing the Fermi node state. The energy dispersions determined by ARPES with several photon energies are superimposed. **(e)** Band dispersion map across Γ point. The energy distribution curves (EDCs) are divided by the Fermi function (FD) at measured temperature (T = 75 K).

parabolic dispersion moves toward E_F with increasing incident photon energy (or increasing $k_{(111)}$), and it eventually touches E_F (see the plots in **Fig. 2d**). As the photon energy is further increased, the dispersion moves away from E_F again, following the quadratic dispersion along $k_{(111)}$. Our data show that the 3D band structure of $Pr_2Ir_2O_7$ has the theoretically predicted Fermi point at the momentum reached by $h\nu \sim 52$ eV, which is thus assigned to be Γ (**Fig. 2b**). Other scans of different $k_{(111)}$ values up to the L point in the Brillouin zone, which is reached at $h\nu$ = 39 eV (**Fig. 2c**), revealed no other states touching or crossing E_F. This absence of other bands crossing E_F is another consistency condition on the Fermi node model, which requires this situation by state counting and charge neutrality [20].

We also point out that broad spectral weight emerges beyond E_F as seen in the Fermi-function divided image for the 75 K data (arrow in **Fig. 2e**). The related spectral intensity is obtained off Γ, showing an upturn behavior beyond E_F. While the strong suppression of quasiparticle peaks at elevated temperatures prevents us from a definitive determination of the conduction band dispersion, the observation of spectral weight above E_F is compatible with the predicted existence of a quadratic band touching on the unoccupied side (**Fig. 2d**).

Our results suggest that tuning of a unique quantum critical point between an antiferromagnetic Weyl semimetal and the non-Fermi liquid nodal phase may be possible by alloying or hydrostatic pressure. Correlated topological phases and device applications with iridate films could be accessed by controlling the strain-induced breaking of the cubic crystal symmetry and size quantization (subband formation) in quantum well structures.

REFERENCES

[1] M. Z. Hasa and C. L. Kane, *Rev. Mod. Phys.* **82**, 3045 (2010).
[2] L. Fu, C. L. Kane and E. J. Mele, *Phys. Rev. Lett.* **98**, 106803 (2007).
[3] J. E. Moore and L. Balents, *Phys. Rev. B* **75**, 121306 (2007).
[4] Y. Ando, *J. Phys. Soc. Jpn.* **82**, 102001 (2013).
[5] B. J. Kim, H. Jin, S. J. Moon, J.-Y. Kim, B.-G. Park, C. S. Leem, J. Yu, T. W. Noh, C. Kim, S.-J. Oh, J.-H. Park, V. Durairaj, G. Cao and E. Rotenberg, *Phys. Rev. Lett.* **101**, 076402 (2008).
[6] Y. Machida, S. Nakatsuji, S. Onoda, T. Tayama and T. Sakakibara, *Nature* **463**, 210 (2009).
[7] W. Witczak-Krempa and Y. B. Kim, *Phys. Rev. B* **85**, 045124 (2012).
[8] D. Pesin and L. Balents, *Nature Phys.* **6**, 376 (2010).
[9] W. Witczak-Krempa, G. Chen, Y.-B. Kim and L. Balents, *Annual Review of Condensed Matter Physics* **5**, 57 (2014).
[10] E.-G. Moon, C. Xu, Y. B. Kim and L. Balents, *Phys. Rev. Lett.* **111**, 206401 (2013).
[11] X. Wan, A. M. Turner, A. Vishwanath and S. Y. Savrasov, *Phys. Rev. B* **83**, 205101 (2011).
[12] D. Yanagishima and Y. Maeno, *J. Phys. Soc. Jpn.* **70**, 2880 (2001).
[13] K. Matsuhira, M. Wakeshima, R. Nakanishi, T. Yamada, A. Nakamura, W. Kawano, S. Takagi and Y. Hinatsu, *J. Phys. Soc. Jpn.* **76**, 043706 (2007).
[14] S. Nakatsuji, Y. Machida, Y. Maeno, T. Tayama, T. Sakakibara, J. van Duijn, L. Balicas, J. N. Millican, R. T. Macaluso and J. Y. Chan, *Phys. Rev. Lett.* **96**, 087204 (2006).
[15] Y. Machida, S. Nakatsuji, Y. Maeno, T. Tayama, T. Sakakibara and S. Onoda, *Phys. Rev. Lett.* **98**, 057203 (2007).
[16] Y. Tokiwa, J. J. Ishikawa, S. Nakatsuji and P. Gegenwart, *Nature Mat.* **13**, 356 (2014).
[17] K. Sun, H. Yao, E. Fradkin and S. A. Kivelson, *Phys. Rev. Lett.* **103**, 046811 (2009).
[18] B. A. Bernevig, T. L. Hughes and S.-C. Zhang, *Science* **314**, 1757 (2006).
[19] C. Brüne, C. X. Liu, E. G. Novik, E. M. Hankiewicz, H. Buhmann, Y. L. Chen, X. L. Qi, Z. X. Shen, S. C. Zhang and L. W. Molenkamp, *Phys. Rev. Lett.* **106**, 126803 (2011).
[20] T. Kondo, M. Nakayama, R. Chen, J. J. Ishikawa, E.-G. Moon, T. Yamamoto, Y. Ota, W. Malaeb, H. Kanai, Y. Nakashima, Y. Ishida, R. Yoshida, H. Yamamoto, M. Matsunami, S. Kimura, N. Inami, K. Ono, H. Kumigashira, S. Nakatsuji, L. Balents and S. Shin, *Nat. commun.* **6**, 10042 (2015).

BEAMLINE

BL-28A

T. Kondo[1], M. Nakayama[1], R. Chen[2, 3], J. J. Ishikawa[1], E.-G. Moon[2, 4], T. Yamamoto[1], Y. Ota[1], W. Malaeb[1, 5], H. Kanai[1], Y. Nakashima[1], Y. Ishida[1], R. Yoshida[1], H. Yamamoto[1], M. Matsunami[6, 7], S. Kimura[6, 8], N. Inami[9], K. Ono[9], H. Kumigashira[9], S. Nakatsuji[1, 10], L. Balents[11] and S. Shin[1]
([1]The Univ. of Tokyo, [2]Univ. of California, [3]LBNL, [4]KAIST, [5]Beirut Arab Univ., [6]IMS, [7]Toyota Tech. Inst., [8]Osaka Univ., [9] KEK-IMSS-PF, [10]JST, [11]KITP)